

Comparison of Adsorption Capacity of Amine Modified Activated Carbon from Stone Apple for CO₂ Capture

Dipa Das (✉ dipadas@igitsarang.ac.in)
Indira Gandhi Institute of Technology (IGIT)

Research Article

Keywords: Activated carbon, Ethylene diamine, Tetra ethylene penta amine, Adsorption, Carbon dioxide

Posted Date: August 8th, 2023

DOI: <https://doi.org/10.21203/rs.3.rs-3228797/v1>

License:  This work is licensed under a Creative Commons Attribution 4.0 International License.
[Read Full License](#)

Abstract

Increase in atmospheric Carbon dioxide concentration due to industrial activity of more than a century has led to the problem of global warming, which hints at a catastrophic climatic consequence for the whole world. The reduction in the emissions of greenhouse gases possesses a challenge in addressing the issue of climate change. Adsorption is considered as a competitive solution. This present research focus separation of post combustion capture carbon dioxide from flue gas by adsorption mechanism as it needs less energy and amine modified activated carbon prepared from stone apple can be used as solid adsorbents. Two different amine solution i.e Ethylene Diamine(EDA) and Tetra Ethylene Penta Amine(TEPA) solution were used as impregnating agent for activated carbon with impregnation ratio 0.4 (EDA-AC(0.4) and TEPA-AC(0.4)). Further the amine impregnated activated carbons were characterized using various techniques such as Proximate Analysis, Ultimate Analysis, Scanning Electron Microscopy (SEM), Energy Dispersive Spectroscopy(EDS), Fourier Transform Infrared spectroscopy(FTIR), BET surface area analyser, Thermo Gravimetric Analysis (TGA), X-Ray Diffraction(XRD). A remarkable increase in the adsorption capacity was observed and the maximum adsorption (36.05 mg/g) is found in Ethylene diamine impregnated activated carbon having impregnation ratio 0.4(EDA-AC(0.4)) at 25°C and 1 atm and break through time of 214 min.

1. Introduction

CO₂ is responsible for global warming which hints at a catastrophic climatic consequence for the whole world, causing the Earth's temperature to rise and resulting in a range of negative impacts on the planet's climate and ecosystems [1, 2]. One of the imminent ways of controlling the problem is capturing the carbon dioxide gas at large industrial source points. The thermal power plants relying on coal burning are the major producers of carbon dioxide. The flue gas from the stacks of such plants usually contains around 10–15% CO₂ by volume. Several technological strategies with different levels of maturity have been tried by scientists and engineers. The amine-based gas-liquid reactive absorption technique used by several thermal power plants is at highest level of technology maturity, but it suffers from exorbitant energy penalty and environmental concern. This present research focus on capture of Carbon dioxide from powerplants using post combustion capture strategy. There are several methods available for capturing CO₂, including cryogenic distillation, absorption, and molecular sieve but these are expensive and energy-intensive. Solid-gas adsorption technique is the most effective CO₂ separation technique from flue gas as it needs less energy and also cost effective[3–6]. To improve the competitiveness of the CO₂ capture process, it is essential to develop new and highly efficient solid adsorbents. There is a plethora of material like membranes, zeolites, polymers, and activated carbon etc. which are examined for their suitability to be used as adsorbent. Activated carbon outperforms the other advanced materials in terms of ease of availability, low cost, moisture resistance, selectivity, Microporous structure and large specific surface area[7–9]. A lot of micropores are present in the activated carbon. The necessity for activated carbon is increasing daily because environmental pollution is today's biggest issue. The source material and the preparation technique have an impact on its surface qualities and texture[5]. Activated carbons

are easily regenerate, no requirement of moisture removal and adsorption capacity of CO₂ is very high at ambient pressure[10]. Both physical and chemical activation processes can be used to create activated carbon[11]. Carbonaceous raw materials are used for preparation of activated carbon like wood, coal, rice husk[12–13], nut shells[14] coconut shells[15], green coconut shell[9], Corncobs[16] pea nuts[17], sugarcane bagasse[18], tamarind wood[13], sawdust[19], sun flower straw[20] and industrial waste products. The impact of various chemical reagents on the prepared activated carbon have been studied by various researchers [19, 21]. Pore structure becomes prominent in chemical activation than physical activation. KOH plays a vital role in the chemical activation process, which converts the precursor material into activated carbon. Activation involves the removal of impurities and the development of a porous structure with a large surface area. KOH acts as a chemical activator that reacts with the precursor material, leading to the formation of pores and increasing the surface area [22–23]. Stone Apple shell was chosen for this study for AC preparation. It contains little ash and a lot of fixed carbon. Small microspore structure leads to more effective adsorption of gas. Activated carbon's adsorption behaviors not only influenced by its porous structure but also by the functional group present on its surface. Porosity determines adsorption capacity and the polar and nonpolar structures of the adsorbate have an impact on the functional group that is present on the surface[24–25]. Biomass residue prepared adsorbent and pre-activated with CO₂ shows differences in texture and surface chemistry significantly which leads to higher capacities as compared to starting char[11].The enhancement of CO₂ capture capacity of the adsorbents depends upon nitrogen functional group[26]. There are some draw backs in simple activated carbon. The adsorption capacity and the selectivity for carbon dioxide is poor at high temperatures. Amine impregnation on the surface of the adsorbents enhances the adsorption capacity of adsorbents for removal of carbon dioxide[27–28]. Due to the presence of amine group, amine impregnated activated carbon offers more adsorption [29–33, 6].

The above discussion points to a lack of studies in literature on attempt to precisely engineer the adsorption surface. In our present research work Ethylene diamine impregnated activated carbon (EDA-AC) and Tetra ethylene penta amine (TEPA-AC) impregnated activated carbon have been prepared with impregnation ratio 0.4 from stone apple shell and study of their CO₂ adsorption capacity in batch adsorption analysis.

2. Material and Methods

2.1. Material and Chemicals

The Stone Apples were collected from the college campus of IGIT Sarang and was used as the raw material for preparation of activated carbon (Fig. 1). Chemical Reagent like Potassium hydroxide (KOH),Ethylene diamine(EDA) and Tetra ethylene penta amine (TEPA),Hydrochloric acid(HCl) were used. Collected stone apples were washed with the normal water to remove the dirt and dust from it. Stone apples were broken for removal of inner flesh of the fruits and left with only outer shell of it. Further the stone apples were broken to small pieces and washed properly with water. Washed Stone Apples were

kept under Sunlight for 3–4 weeks for drying and removal of outer moisture (Fig. 2). The dried materials were heated to 105°C for 24 hours in the Hot air oven for removal of other volatile matter and moisture. It was then crushed using Iron Pestle and Mortar and sieved to average size range of 300–425 μ m.

2.2. Preparation of Adsorbents

KOH was used to chemically activate the powdered stone apple shell, with an impregnation ratio of 1:1 (activating agent/precursor) (20 g of the dry powder was thoroughly mixed with 80 ml of KOH solution). The impregnation ratio was calculated using the Eq. (1). The slurry of the precursor powder was thoroughly mixed and stored for 24 hours for proper soaking of KOH. The slurry was kept in the hot air oven (Fig. 3) for 24 hours at 105°C. KOH was used as an impregnating agent for the preparation of activated carbon because it helps to increase the surface area and more micropores and mesopores to enhance its adsorption properties [34]. KOH impregnated samples were kept inside the muffle furnace within a galvanised iron pipe with the following measurements: Outer diameter 5 cm, Length 20 cm and thickness .05 cm. (Fig. 4). The material was inside the furnace at 650°C for one hour under the flow of nitrogen (150 cm³ min⁻¹ STP), After that, it was chilled until it was entirely cooled under the continuous flow of nitrogen gas. To eliminate various remaining organic and mineral impurities, the dry material was washed with 0.5 N HCl followed by warm distilled water. The final step was washing it in cold water until the solution became neutral (pH range 6.0 to 7.0). The sample was then sealed in an airtight container after drying for 24 hours at 105°C in an oven. Further the prepared Activated Carbon was impregnated with Ethylene Diamine solution and Tetra Ethylene Penta Amine in the impregnation ratio of 0.4 resulting in to amine impregnated activated carbon of EDA-AC (0.4) (Fig. 5) and TEPA-AC(0.4) (Fig. 6).

$$\text{Impregnation Ratio (IR)} = \text{KOH weight/Dried precursor weight} \quad \text{--- (1)}$$

2.3. Characterization of Adsorbents

Proximate analysis and ultimate analysis of the raw precursor and amine impregnated activated carbon adsorbents were carried out. Textural Characteristics of the adsorbents were determined by Brunauer-EmmettTeller (BET) analyser. Thermogravimetric analyses of the prepared adsorbents were carried out to check its thermal stability of the adsorbent material. The surface functional groups of adsorbents were analyzed using Fourier transform infra-red (FTIR) spectroscopy. SEM-EDS analyzer was used to analyze the surface morphology and elemental analysis of the prepared amine impregnated activated carbon adsorbents. XRD analysis was used to check the crystallographic structure of prepared adsorbent samples. CO₂ adsorption analysis was done by Autosorb iQ manufactured by Quanta chrome Quanta chrome Instruments to find out the carbon dioxide adsorption capacity of the prepared samples.

3. Results and Discussion

3.1 Proximate Analysis

Proximate analysis is the study and analysis of a sample, defining the numerous compositions such as % moisture content, % volatile matter content, % ash content, and % fixed carbon content. Table 1 provides the results of the proximate analysis. According to this study, the fixed carbon content of EDA-AC (0.4), TEPA-AC (0.4), and AC was very high when compared to raw precursor, resulting in a better adsorbent for adsorption purposes. As the fixed carbon content increases, the % moisture content, % volatile moisture content, % ash content falls. These tests revealed that the precursor's highly volatile matter and low ash content made it an excellent starting material for the synthesis of activated carbon[35–37, 24]. The fixed carbon content in the raw precursor material was 43.12%, but when the material was activated, fixed carbon content increases to 76.18%. The fixed carbon content value again changed from 76.18–72.43% after the activated carbon had been impregnated with EDA solution at a impregnation ratio of 0.4 and it changed from 76.18–71.09% for TEPA-AC (0.4).

Table 1
Proximate Analysis of Raw Precursor, AC and EDA-AC (0.4) and TEPA-AC (0.4)

Sample	Moisture Content (%)	Volatile Matter (%)	Ash Content (%)	Fixed Carbon (%)
Raw	13.56	40.2	3.12	43.12
AC	3.38	19.54	0.89	76.18
EDA-AC (0.4)	4.42	21.84	1.31	72.43
TEPA-AC (0.4)	4.86	22.28	1.75	71.09

3.2. Ultimate Analysis

The determination of elemental composition of the prepared adsorbents were determined by Ultimate analysis. The results of the ultimate analysis are shown in Table 2. From this analysis, it has been found that the percentage of carbon increases in AC after activation and carbonization process [35] and also, it has been observed the percentage of nitrogen was more in EDA-AC (0.4) and TEPA-AC (0.4) due to impregnation of amine solution on the surface of activated carbon, so ultimately the carbon content decreases. The production of activated carbon from Stone Apple shell involves the processes of pyrolysis and activation, which cause a reduction in the levels of hydrogen, nitrogen, sulphur, and oxygen. This is due to the decomposition of the stone apple shell, which results in the release of volatile compounds primarily containing H₂, O₂, and N₂. As a result, the remaining carbonaceous material becomes enriched in carbon, leading to an increase in the carbon content of the final activated carbon product. Because KOH removed the H and O from the Stone Apple shell as H₂O and H₂ instead of CO, CO₂, or Hydrocarbons[36, 38].From Table 2, it has been seen that the carbon content of Raw Precursor was 42.25% but after activation it has risen from 42.25–75.93% in AC, but when the Activated Carbon was impregnated with a EDA-AC (0.4), the Carbon % decreased from 75.93–70.53% in case of EDA-AC(0.4)and the Carbon % decreased from 75.93–69.15% in the case of TEPA-AC (0.4).There has been a decrease in the Hydrogen and Sulphur content from 9.40–1.065% and 33.26–0.72%, respectively. There has been an increase in Hydrogen content from 1.06–2.87% for EDA-AC (0.4) also increase in Hydrogen

content from 1.06–3.35% for TEPA-AC(0.4). Due to release of volatile matter, the percentage of carbon content in all the activated samples were increases. The percentage of nitrogen in the raw precursor and activated carbon is 3.19% and 1.65%. After amine impregnation the percentage of nitrogen in EDA-AC(0.4) was 5.71% and TEPA-AC(0.4) was 4.87%. The nitrogen content was more in the amine impregnated samples.

Table 2
Ultimate Analysis of Raw Precursor, AC and EDA-AC(0.4) and TEPA-AC(0.4)

Sample	Nitrogen (%)	Carbon (%)	Hydrogen (%)	Sulfur (%)	Oxygen (%)
Raw	3.19	42.25	9.40	33.26	11.90
AC	1.65	75.93	1.06	0.72	20.64
EDA-AC (0.4)	5.71	70.53	2.87	0.30	20.59
TEPA-AC (0.4)	4.87	69.15	3.35	0.98	21.65

3.3 Textural Characteristics of Adsorbents

Adsorption is greatly aided by micropores. The textural properties of the EDA-AC(0.4) and TEPA-AC(0.4) were characterized by measuring the nitrogen adsorption/desorption isotherms at 77 K. Figure 7(a) and Fig. 8(a) shows the nitrogen adsorption capacity with respect to the nitrogen relative pressure (P/P_0) of EDA-AC(0.4) and TEPA-AC(0.4) treated at 650°C for 60 min. At low pressure it was observed that there is a sharp increase in pore volumes for the both amine impregnated activated carbons which is the indicator of the presence of a more amount of micropores present in the adsorbents[39]. Figure 7(b) and (c) and Fig. 8(b) and (c) shows the pore size distribution curve for EDA-AC (0.4) and TEPA-AC(0.4) respectively. Nitrogen adsorption was greater in amine impregnated activated carbon than in raw precursor due to micropores formed during activation and carbonization Total pore volume of the adsorbents is defined as the volume of liquid nitrogen adsorbed at a relative pressure (P/P_0) of 0.99 [40]. The results of the BET Surface Area and pore structure parameters were shown in Table 3. According to the Table 3, the presence of micropores in Stone Apple shell is nil, resulting in the least Nitrogen adsorption. The shape of the adsorption isotherm's determines the adsorption mechanism as well as the carbon's pore structure. These isotherms are classified as Type I by IUPAC, which represents dense micropore structures [24]. Under optimal circumstances, the surface area and pore volume of Raw Precursor were $57.813\text{ m}^2/\text{g}$ and $0\text{ cm}^3/\text{g}$, respectively. The average pore radius of Raw Precursor was 14.945 \AA . The surface area and micro pore volume of Activated Carbon, respectively, were $991.653\text{ m}^2/\text{g}$ and $0.369\text{ cm}^3/\text{g}$ under ideal conditions. Surface area and pore volume after being impregnated with the EDA solution at a ratio of 0.4 were $738.481\text{ m}^2/\text{gm}$ and $0.302\text{ cm}^3/\text{gm}$, respectively, while they were $714.401\text{ m}^2/\text{gm}$ and $0.294\text{ cm}^3/\text{gm}$ for TEPA-AC(0.4). It was discovered to be considerably high when compared to raw precursor and activated carbon, indicating stronger adsorbent properties. According to the literature, adsorption performance is more when the specific surface area of the adsorbent is higher[41].

Table 3
Pore structure parameter of Raw precursor, AC, EDA-AC (0.4) and TEPA-AC(0.4)

Sample	BET SSA(m ² /gm)	T _{Tot} (cm ³ /gm)	V _{Micro} (cm ³ /gm)	A _{Micro} (m ² /gm)	Avg. Pore radius (Å°)
Raw precursor	57.813	0.06341	0	0	14.945
AC	991.653	0.438	0.369	923.52	9.213
EDA-AC (0.4)	738.481	0.397	0.302	709.32	8.431
TEPA-AC (0.4)	714.401	0.349	0.294	693.43	7.518

3.4 SEM-EDS Analysis

SEM-EDS analysis is required to find out the microstructural characterization of materials. It gives the information about the identification of which elements are present in the sample and the amount of each element [42–43]. The basic principle of EDS is a generation of X-rays from a specimen through the electron beam. Energy Dispersive X-ray Spectroscopy (EDS) images providing a combined morphological and chemical overview of the sample and chemical composition of a sample for elements with atomic number. EDS works by using an electron microscope to emit a focused scanning electron beam, exciting the sample's atoms, so they emit characteristic spectrums of x-rays. The surface of the EDA impregnated Activated Carbon and TEPA impregnated activated carbon sample is exposed to a high-energy electron beam during the SEM investigation. To produce a high-resolution image of the surface, signals produced by the interaction of the electrons with the sample must be detected. Information on the size, shape, and distribution of the pores and particles on the surface of the activated carbon is revealed by the image that is produced. Figures 9 and 10 shows the SEM-EDS micrographs of EDA-AC (0.4) and TEPA-AC (0.4) made at 650°C for 1 hour. Different pores were seen in the sample of amine impregnated activated carbon. Volatiles are eliminated during carbonization and activation, resulting in a fixed carbon mass and a widening of the pore networks in the activated carbon sample. The existence of micropores aids in the adsorption of gases[44]. From EDS analysis it has been seen that there are different element like Carbon(C),Nitrogen(N),Oxygen(O),Aluminium(Al) ,Silicon(Si), Sulphur(S), Chlorine(Cl) and Zinc(Zn) present. From the Tables 4,5,6 and 7 it has been seen that the weight percentage of carbon is much more than that of other elements. The weight percentage of carbon for EDA-AC(0.4) of 10 Micron Magnification is 68.6% and of 68.8% for 70 Micron Magnification. Similarly The weight percentage of carbon for TEPA-AC(0.4)of 60 Micron Magnification is 53.18% and of 54.67% for 30 Micron Magnification.

Table 4
EDS analysis of EDA-AC (0.4) (10
Micron Magnification)

Element	Weight(%)	Atomic(%)
C	68.6	77.02
N	6.06	5.84
O	16.11	13.58
Al	2.28	1.14
Si	1.94	0.93
S	0.25	0.1
Cl	2.3	0.87
Zn	2.46	0.51

Table 5
EDS analysis of EDA-AC (0.4) (70
Micron Magnification)

Element	Weight (%)	Atomic (%)
C	68.8	75.56
N	10.5	9.89
O	15.66	12.91
Al	0.31	0.15
Si	0.02	0.01
S	0.2	0.08
Cl	2.84	1.06
Zn	1.67	0.34

Table 6
EDS analysis of TEPA-AC(0.4) (60 Micron Magnification)

Element	Weight(%)	Atomic(%)
C	53.18	61.23
N	14.22	14.04
O	25.15	21.73
Al	1.2	0.61
Si	2.07	1.02
S	0.22	0.09
Cl	2.43	0.95
Zn	1.54	0.33

Table 7
EDS analysis of TEPA-AC (0.4) (30 Micron Magnification)

Element	Weight(%)	Atomic(%)
C	54.67	65.75
N	6.76	6.97
O	23.46	21.18
Al	7.59	4.07
Si	0.17	0.09
S	0.18	0.08
Cl	1.49	0.61
Zn	5.68	1.26

3.5 Fourier Transform Infrared (FTIR)

The FTIR is used to analyze the surface chemistry of various materials and detection of the functional groups present in the sample by measuring the vibration frequencies of atoms in molecules, which depend on their mass and bond strength. Bonds absorb radiation in the infrared area of the electromagnetic spectrum, which stimulates molecular vibrations. All kinds of functional groups like Carboxylic, carbonyl, phenol, and lactone and amine functional groups are present in the samples Fig. 11 and Fig. 12 shows the FTIR graph of EDA-AC(0.4) and TEPA-AC(0.4). The existence of an O-H bond, alcohol, phenol functional group are indicated by the range $3500 - 3200 \text{ cm}^{-1}$. Presence of N-H bond at

1400 cm^{-1} . C-O stretching vibration in hydroxyl and phenol groups causes a band at 1100 cm^{-1} . The carboxylic groups and alkanes (C-H bond) can be seen in the frequency range 1750 and 1100 cm^{-1} and $1470 - 1450\text{ cm}^{-1}$.

3.6 Thermo Gravimetric Analysis (TGA)

TGA analysis provides the thermal behavior of the prepared adsorbents. The original weight vs temperature and weight vs time plot for DEA-AC(0.4) and TEPA-AC(0.4) is shown in the graphs Fig. 13 and Fig. 14. When temperature increases from 27°C to 800°C , it has been noticed that the percentage of weight loss for EDA-AC (0.4) was 32.465% and the percentage of weight loss for TEPA-AC (0.4) was 34.146%. As a result, EDA-AC (0.4) is considered as a good adsorbent because of its excellent heat stability. When closely examined, both graphs displayed the same tendencies. Three steps can be distinguished between two graphs. The highest lowering slope occurred in the first step, which showed 5.024% of weight loss for EDA-AC (0.4) for the temperature range 27°C to 150°C and showed 4.273% of weight loss for TEPA-AC (0.4) for the temperature range 27°C to 150°C due to the removal of volatile substances, moisture, and other contaminants. As the organic substance breaks down, gaseous volatiles are released[45]. The second stage's decreasing slope was slightly less steep, which showed weight loss of 19.23% of EDA-AC(0.4) for the temperature range from 150°C - 450°C and weight loss 22.65% was seen in the TEPA-AC (0.4) for the temperature range from 150°C - 410°C . In the third stage, the graph showed the weight loss of 8.211% for the temperature range from 450°C - 800°C , and weight loss of 7.223% was seen in the TEPA-AC(0.4) for the temperature range from 410°C - 800°C . By comparing the two plots, it has been found that from room temperature to 800°C , EDA-AC (0.4) has a very strong resistance to weight loss compared to TEPA-AC (0.4) for same rise in temperature. As a result, EDA impregnated Activated Carbon can withstand temperatures of up to 800°C without suffering a substantial weight loss.

3.7 X-Ray Diffraction (XRD)

XRD analysis is used to determine the crystallographic structure of material. XRD graph for DEA-AC(0.4) and TEPA-AC(0.4) is shown in Fig. 15 and Fig. 16. It can be seen from the graph that there is absence of sharp peak in Ethylene diamine impregnated activated carbon (EDA-AC(0.4)) and in Tetra ethylene penta amine impregnated activated carbon (TEPA-AC(0.4)) which indicates that the amine impregnated materials are primarily amorphous structure, which is a favorable characteristic for good adsorbents. EDA-AC (0.4) shows peak 24° at and TEPA- AC(0.4) shows at 22° .

3.8 CO₂ Adsorption Analysis

The autosorb iQ instrument (Fig. 17) manufactured by Quanta chrome was used for CO₂ adsorption analysis. The adsorption of CO₂ in this experiment was carried out until the relative pressure (air pressure to atmospheric pressure) reached 1 bar [6]. The sample was exposed to atmospheric pressure for 6 hours while being out gassed at 523K. The CO₂ adsorption of the sorbents at relative pressure (P/P_0) was evaluated at 298 K after degassing, under a vacuum. The CO₂ adsorption capacity and the volume of the CO₂ adsorbed for EDA-AC(0.4) and TEPA-AC(0.4) is plotted against relative pressure as shown in the

Fig. 18 and Fig. 19. From Fig. 18 graph, it has been seen that the carbon dioxide adsorption capacity of EDA-AC(0.4) was 35.77 mg/g and volume of carbon dioxide adsorbed was 18.21 cc/g. From the Fig. 19 it has been seen that the carbon dioxide adsorption capacity of TEPA-AC(0.4) was 16.37 mg/g and volume of carbon dioxide adsorbed was 8.33 cc/g. EDA-AC (0.4) has a higher carbon dioxide adsorption capacity i.e. 35.77 mg/g and high volume of carbon dioxide adsorbed than TEPA-AC (0.4). Amines are a significant source of acidic carbon dioxide gas adsorption base sites. Because of its acid-base characteristics, amine on the AC surface boosts carbon dioxide adsorption capacity and selectivity. CO_2 is Lewis acid, while amines are Lewis base. A lone pair of electrons is present on a nitrogen atom in an amine functional group. Thus, there is a nucleophilic attack on acidic carbon dioxide, resulting in carbamate production via the carboxyl group[46, 47]. The graph shows that the EDA-AC (0.4) has a larger carbon dioxide adsorption capacity than the TEPA-AC (0.4) sample due to the action of chemisorption. Because of its fast reaction kinetics and high adsorption capacity, EDA-AC (0.4), as an alkyl amine, has two amine groups in each single molecule and is employed as an activator to boost CO_2 adsorption performance [48–50]. Viscosity of EDA and TEPA are 1.7 cSt and 54.1 cSt at 25 °C respectively. EDA is of less viscous than TEPA that affects the CO_2 reaction to a greater extent.

3.9 Breakthrough curve of CO_2 for Adsorbents

The breakthrough curve of CO_2 adsorption for amine impregnated activated carbon (EDA-AC(0.4) and TEPA-AC(0.4)) has been shown in Fig. 20. It has been observed from the breakthrough curve that EDA impregnated activated carbon have a higher carbon dioxide adsorption capacity than TEPA impregnated activated carbon, due to the effect of chemisorption. EDA is of less viscous than TEPA that affects the CO_2 reaction to a greater extent. From these results, EDA-AC may act as better adsorbent than TEPA-AC for CO_2 capture. The maximum adsorption capacity for EDA-AC (0.4) and TEPA-AC (0.4), was found out to be 36.05 and 18.28 mg/g at 214 min and 249 min respectively.

4. Conclusions

The preparation and characterization of amine impregnated activated carbon made from Stone Apple shells has proven to be a highly effective efficient adsorbent material. The process of chemical activation, involving carbonization, enhances the surface area and porosity of the Stone Apple shell-derived activated carbon. The results show that the prepared EDA impregnated activated carbon at a ratio of 0.4 had a high surface area of $738.48 \text{ m}^2/\text{g}$ and a microporous structure with a pore radius of 8.431 \AA^0 and micropore volume $0.302 \text{ cm}^3/\text{g}$. In TEPA impregnated Activated Carbon at a ratio of 0.4 had surface area of $714.4 \text{ m}^2/\text{g}$ and pore radius of 7.52 \AA^0 with micropore volume $0.294 \text{ cm}^3/\text{g}$. The FTIR analysis revealed the presence of various functional groups such as hydroxyl, carboxyl, and phenolic groups and amine groups which enhance the adsorption of CO_2 . From TGA analysis it has been seen that the percentage of weight loss for EDA-AC(0.4) is 32.465% which was less than that of TEPA-AC(0.4) with respect to same change of temperature variation. EDA-AC(0.4) material was more thermal stable than that of TEPA-AC(0.4). The graph depicting the CO_2 adsorption capacity Vs Relative Pressure for EDA-AC

(0.4) and TEPA-AC (0.4), reveals that EDA-AC (0.4) exhibits the highest carbon dioxide adsorption capacity as compared to TEPA-AC (0.4). EDA-AC (0.4) had CO₂ adsorption capacity of 35.77 mg/g and TEPA-AC (0.4) had CO₂ adsorption capacity of 16.27 mg/g at 25°C and 1 atm.. Volume of CO₂ adsorbed for EDA-AC (0.4) is found to be 18.21cc/g and Volume of CO₂ adsorbed for TEPA-AC (0.4) is 8.33 cc/g at 25°C and 1 atm. By examining both graphs, it can be concluded that the activated carbon prepared with EDA impregnation at a ratio of 0.4 acts as a superior adsorbent. The break through time for EDA-AC(0.4) was 214 min with maximum CO₂ adsorption capacity 36.05 mg/g .

Declarations

Funding

This work was supported by OURIIP Seed funding sponsored by OSHEC and Chemical Engineering Department, Indira Gandhi Institute of Technology.Sarang.Odisha.

Competing Interest

The Author has no conflict of interest.

References

1. F. Birol, *Redrawing the energy-climate map: world energy outlook special report* (International Energy Agency, France, 2013)
2. J.A. Church, J.M. Gregory, P. Huybrechts, M. Kuhn, K. Lambeck, M.T. Nhuan, ..., P.L. Woodworth, Climate Change 2001: The Scientific Basis: Contribution of Working Group I to the Third Assessment Report of the Intergovernmental Panel., 639–694. (2001)
3. X. Xu, C. Song, B.G. Miller, A.W. Scaroni, Ind. Eng. Chem. Res. **44**, 8113 (2005)
4. H.J. Fornwalt, R.A. Hutchins, Chem. Eng. **73**, 179 (1966)
5. J. Acharya, J.N. Sahu, B.K. Sahoo, C.R. Mohanty, B.C. Meikap, Chem. Eng. J. **150**, 25 (2009)
6. D. Das, B.C. Meikap, Indian Chem. Eng. **63**, 435 (2021)
7. S. Choi, J.H. Drese, C.W. Jones, ChemSusChem. **2**, 796 (2009)
8. J.N. Sahu, J. Acharya, B.C. Meikap, Bioresour. Technol., 101,1974(2010)
9. D. Das, D.P. Samal, B.C. Meikap, J. Chem. Eng. Process. Technol. **6**, 1000248 (2015)
10. M. Olivares-Marín, C. Fernández-González, A. Macías-García, and V. Gómez-Serrano Appl. Surf. Sci. **252**, 5967 (2006)
11. M.G. Plaza, C. Pevida, B. Arias, J. Fermoso, F. Rubiera, J.J. Pis, A Energy Procedia. **1**, 1107 (2009)
12. K. Mohanty, J.T. Naidu, B.C. Meikap, M.N. Biswas, Ind. Eng. Chem. Res. **45**, 5165 (2006)
13. J.N. Sahu, J. Acharya, B.C. Meikap, J. Hazard. Mater. **172**, 818 (2009)
14. A. Ahmadpour, D.D. Do, Carbon. **35**, 1723 (1997)

15. C.J. Kirubakaran, K. Krishnaiah, & S.K. Seshadri. Ind. Eng. Chem. Res. **30**, 2411 (1991)
16. D. Das, L. Swain, *Advances in Chemical, Bio and Environmental Engineering Cham* (Springer International Publishing., 2022), pp. 219–228
17. K. Periasamy, and C. Namasivayam. Chemosphere. **32**, 769–789 (1996)
18. K.J. Cronje, K. Chetty, M. Carsky, J.N. Sahu, B.C. Meikap, Desalination. **275**, 276 (2011)
19. K. Mohanty, D. Das, M.N. Biswas, Chem. Eng. J. **115**, 121 (2005)
20. L.P. Chen, Y. Jiao, Water Sci. Eng. **16**, 192–202 (2023)
21. V. Fierro, V. Torné-Fernández, A. Celzard, Microporous Mesoporous Mater. **92**, 243 (2006)
22. A.H. Wazir, I.U. Haq, A. Manan, A. Khan, Int. J. Coal Prep Util. **42**, 1477 (2022)
23. B. Doczekalska, M. Bartkowiak, H. Łopatka, M. Zborowska, BioResources. **17**, 1794 (2022)
24. S. Yorgun, N. Vural, H. Demiral, Microporous mesoporous Mater. **122**, 189 (2009)
25. A. Siddiqua, P. Sherugar, D.H. Nagaraju, M. Padaki, J. Energy Storage. **50**, 104698 (2022)
26. C. Pevida, M.G. Plaza, B. Arias, J. Fermoso, F. Rubiera, J.J. Pis, Appl. Surf. Sci. **254**, 7165 (2008)
27. V. Zelenak, D. Halamova, L. Gaberova, E. Bloch, P. Llewellyn, Microporous mesoporous Mater. **116**, 358 (2008)
28. D.I. Jang, S.J. Park, Bull. Korean Chem. Soc. **32**, 3377 (2011)
29. D. Das, D.P. Samal, B.C. Meikap, Environ. Sci. Health. **51**, 769 (2016)
30. D. Das, D.P. Samal, N. Mohammad, B.C. Meikap, Adv. Powder Technol. **28**, 854 (2017)
31. D. Das, B.C. Meikap, Fuel, **224**, 47 (2018.)
32. D. Das, S.K. Behera, B.C. Meikap, Int. J. Coal Sci. Technol. **6**, 445 (2019)
33. D. B.C. Das, Meikap, Min. Process Extr Metall. **130**, 98 (2021)
34. J. Yang, K. Qiu, Chem. Eng. J. **167**, 148 (2011)
35. A. Kumar, H.M. Jena, Appl. Surf. Sci. **356**, 753 (2015)
36. O. Bag, K. Tekin, S. Karagoz, Fuller. Nanotub Carbon Nanostr. **28**, 1030 (2020)
37. Y. Yuliusman, F.A. Farouq, S.P. Sipangkar, M. Fatkhurrahman, S.A. Putri, In AIP Conference Proceedings., 2255, 2020
38. Q. Miao, Y. Tang, J. Xu, X. Liu, L. Xiao, Q. Chen, Taiwan. Inst. Chem. Eng. **44**, 458 (2013)
39. W.C. Lim, C. Srinivasakannan, N. Balasubramanian, J. Anal. Appl. Pyrolysis. **88**, 181 (2010)
40. S. Yorgun, D. Yıldız, J. Taiwan. Inst. Chem. Eng. **53**, 122 (2015)
41. J. Guo, A.C. Lua, Sep. Purif. Technol. **30**, 265 (2003)
42. P.J. Goodhew, J. Humphreys, *Electron microscopy and analysis* (CRC press, 2000)
43. D.C. Bell, A.J. Garratt-Reed, Garland Sci., **49**(2003)
44. A. Khelifi, M.C. Almazán-Almazán, M. Pérez-Mendoza, M. Domingo-García, F.J. López-Domingo, L. Temdrara ... and, A. Addoun, Fuel Process. Technol. **91**, 1338 (2010)
45. T.H. Liou, S.J. Wu, J. Hazard. Mater. **171**, 693 (2009)

46. P.V. Danckwerts, Chem. Eng. Sci. **34**, 443 (1979)
47. M. Caplow, Am. Chem. Soc. J. **90**, 6795 (1968)
48. P. Galindo, A. Schäffer, K. Brechtel, S. Unterberger, G. Scheffknecht, Fuel. **101**, 2 (2012)
49. A. Hartono, E.F. da Silva, H.F. Svendsen, Chem. Eng. Sci. **64**, 3205 (2009)
50. M. Faisal, A.Z. Pamungkas, Y.K. Krisnandi, Processes. **9**, 456 (2021)

Figures



Figure 1

Stone Apple



Figure 2

Dried Crushed Stone Apple



Figure 3

Hot Air Oven



Figure 4

Muffle Furnace



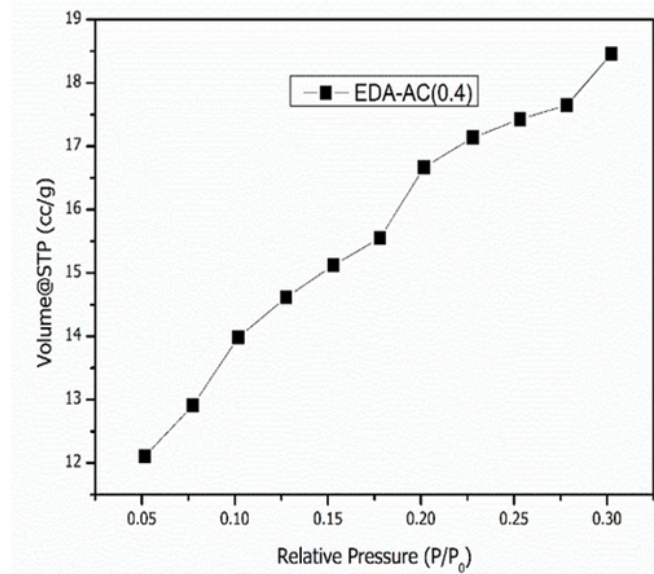
Figure 5

EDA-AC (0.4)

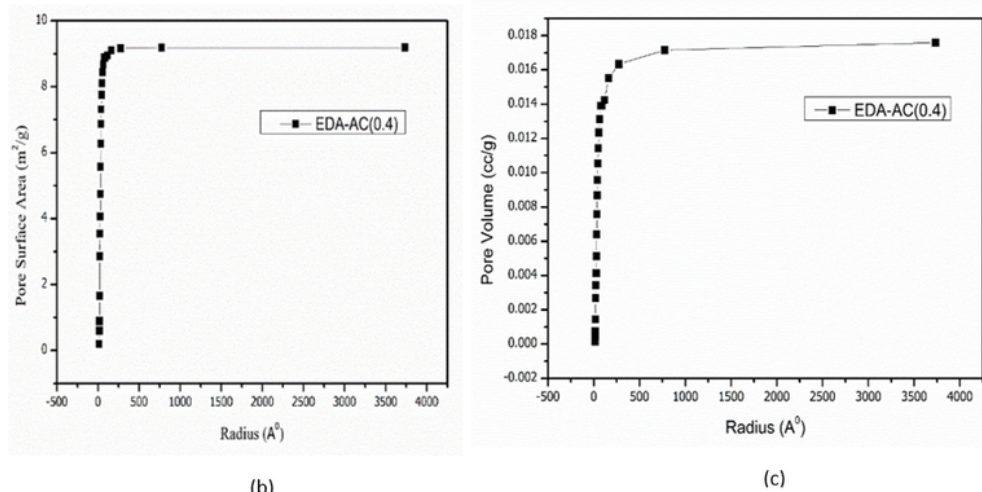


Figure 6

TEPA-AC (0.4)



(a)



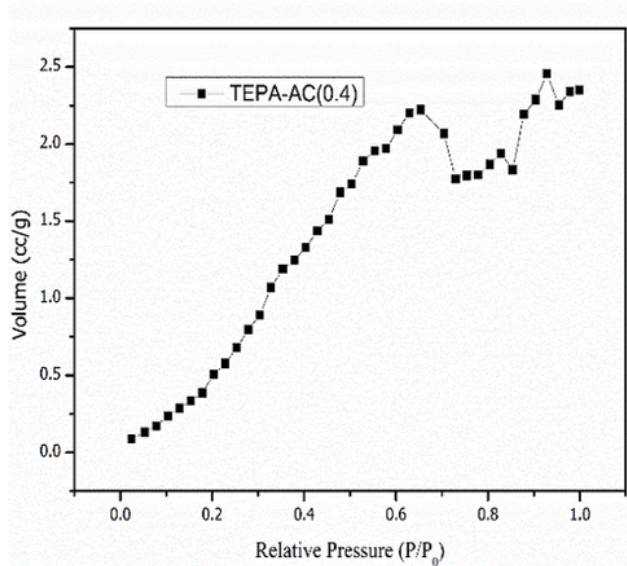
(b)

(c)

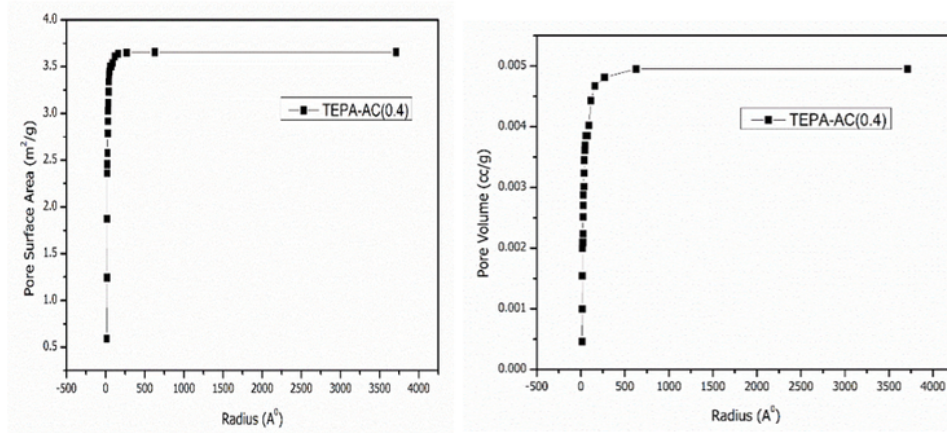
Figure 7

(a) Nitrogen adsorption capacity for TEPA-AC (0.4)

(b)and(c) Pore size distribution for EDA-AC (0.4)



(a)



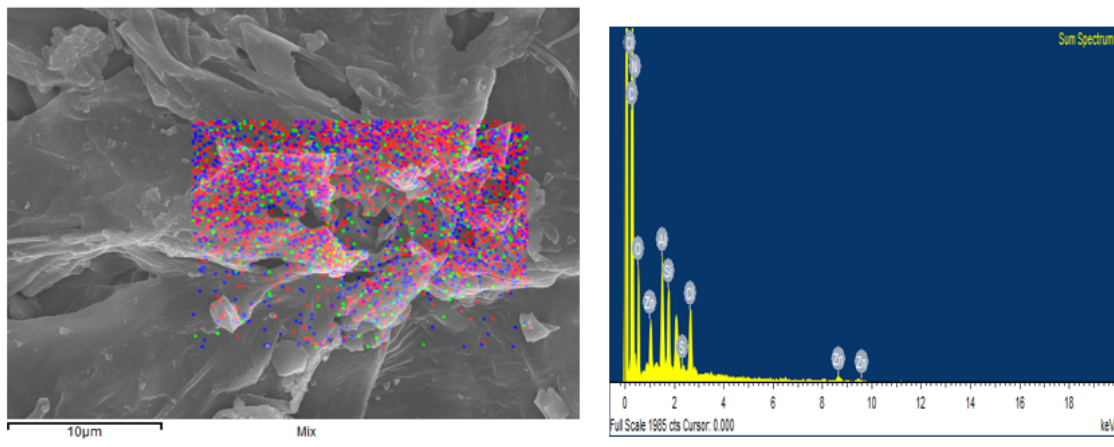
(b)

(c)

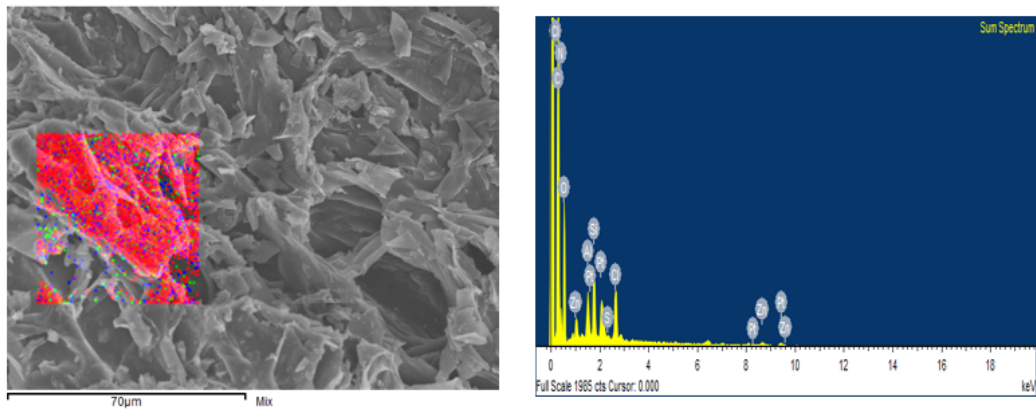
Figure 8

(a) Nitrogen adsorption capacity for TEPA-AC (0.4)

(b)and(c) Pore size distribution for TEPA-AC (0.4)



(a)

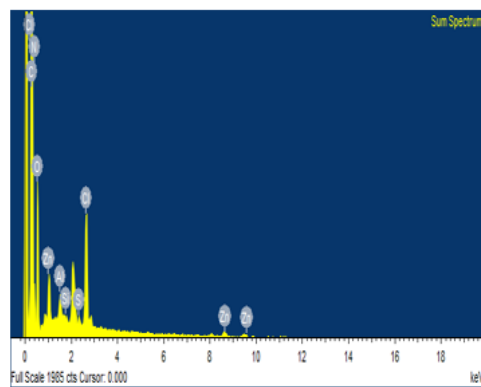
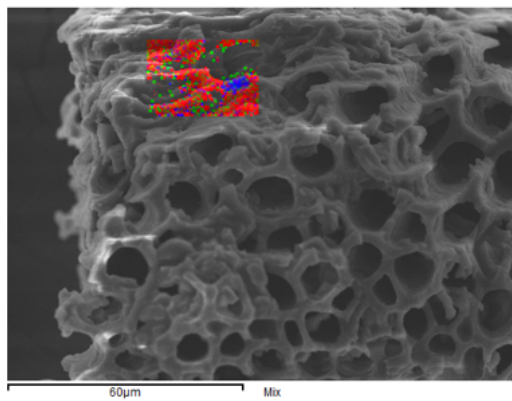


(b)

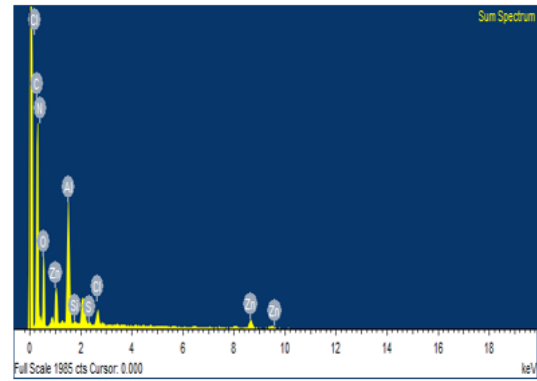
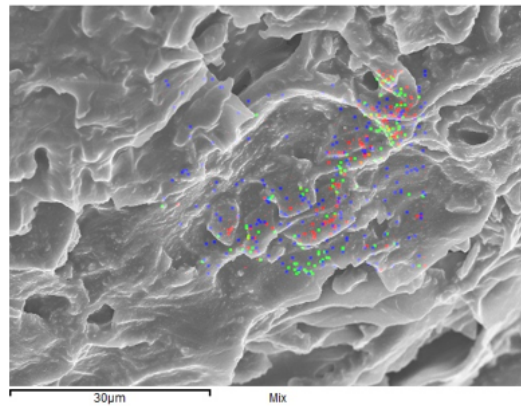
Figure 9

(a) SEM-EDS image for DEA-AC (0.4) of 10 micron magnification

(b) SEM-EDS image for DEA-AC (0.4) of 70-micron magnification



(a)



(b)

Figure 10

(a) SEM-EDS image for TEPA-AC (0.4) of 60 micron magnification

(b) SEM-EDS image for TEPA-AC (0.4) of 30 micron magnification

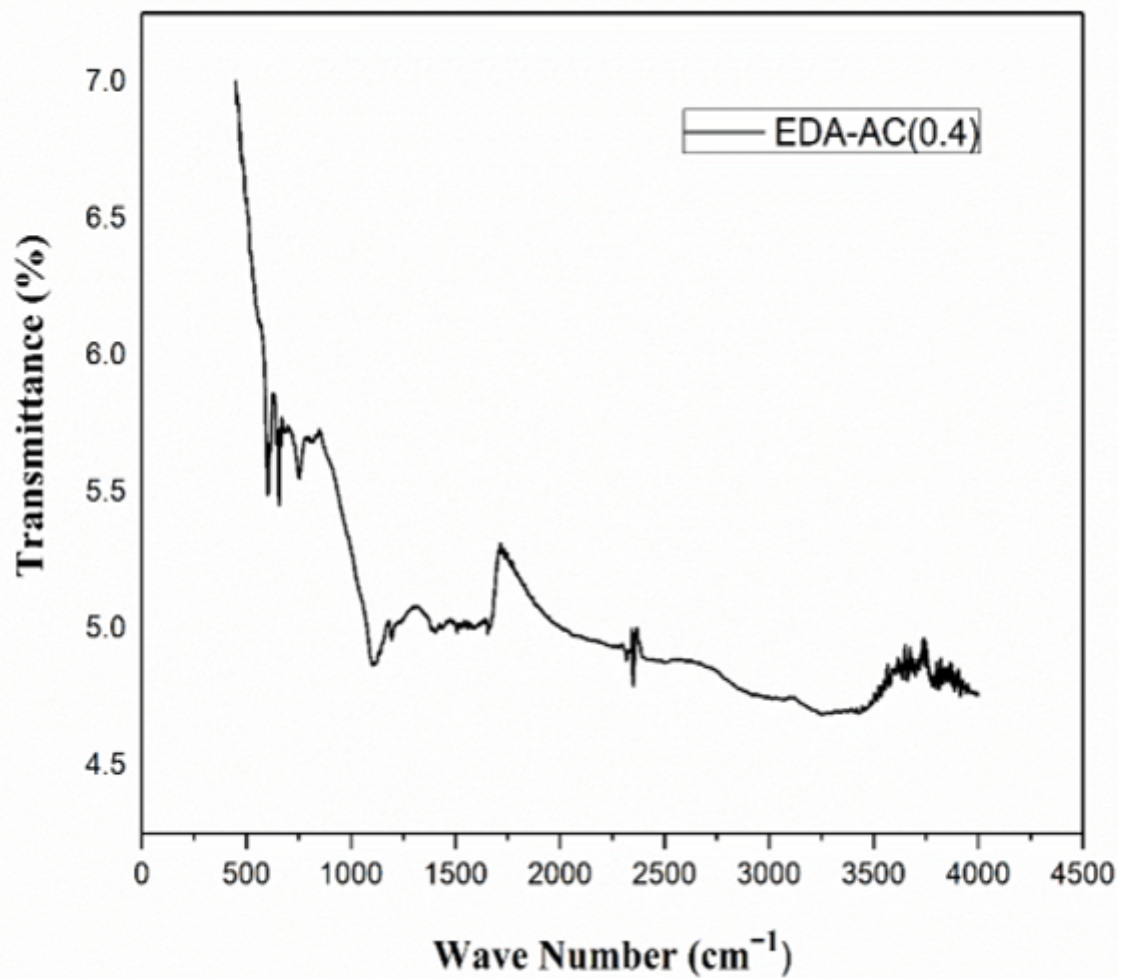


Figure 11

FTIR analysis of EDA-AC (0.4)

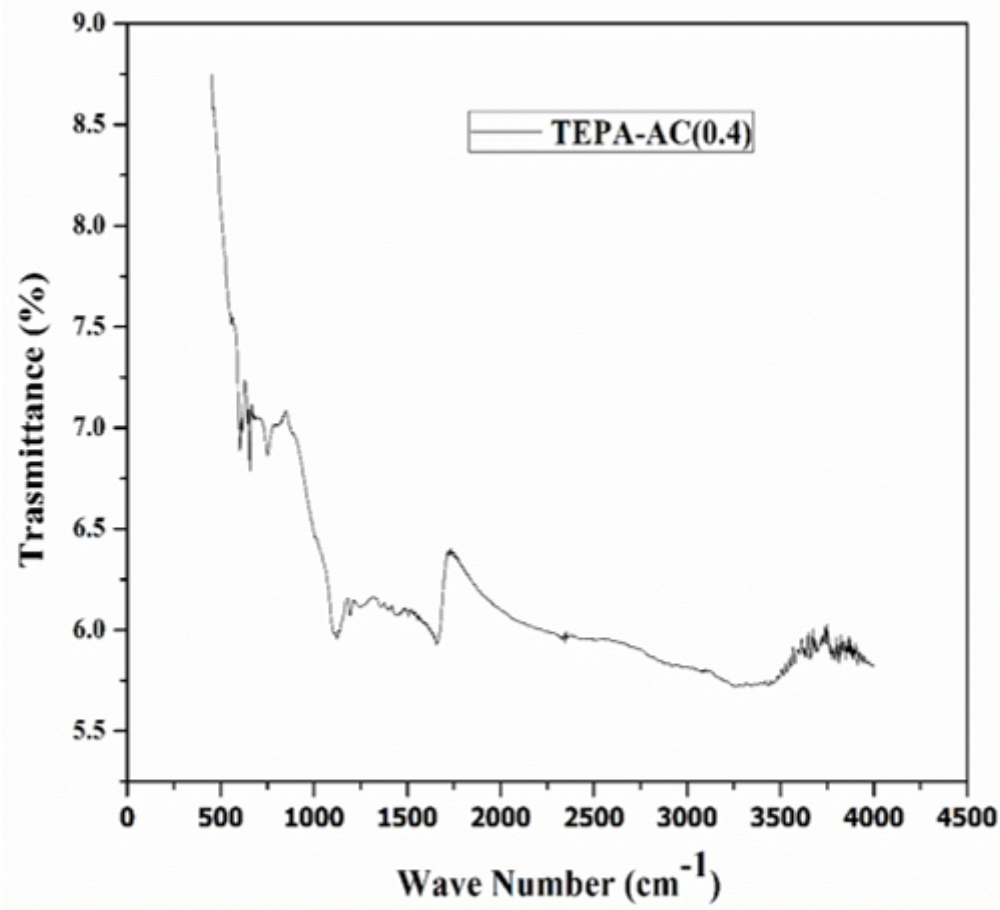
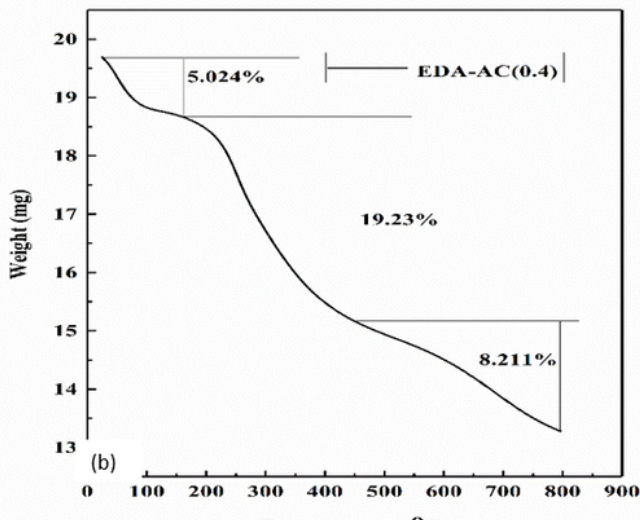
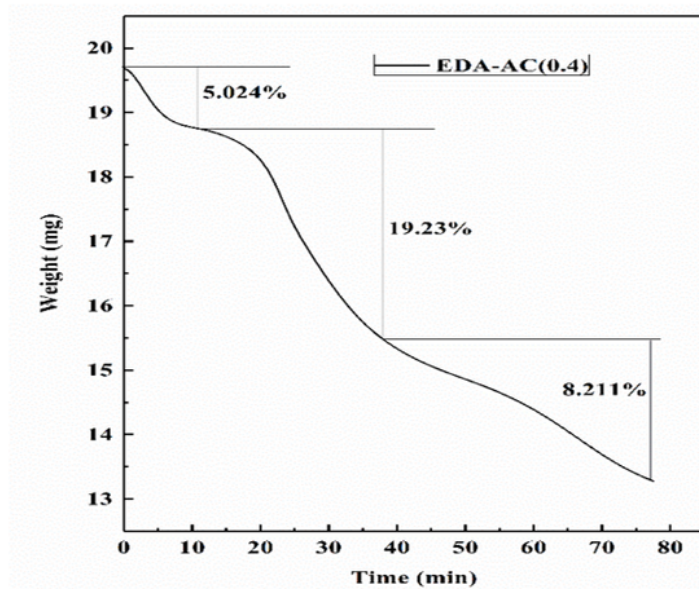


Figure 12

FTIR Analysis of TEPA-AC (0.4)



(a)

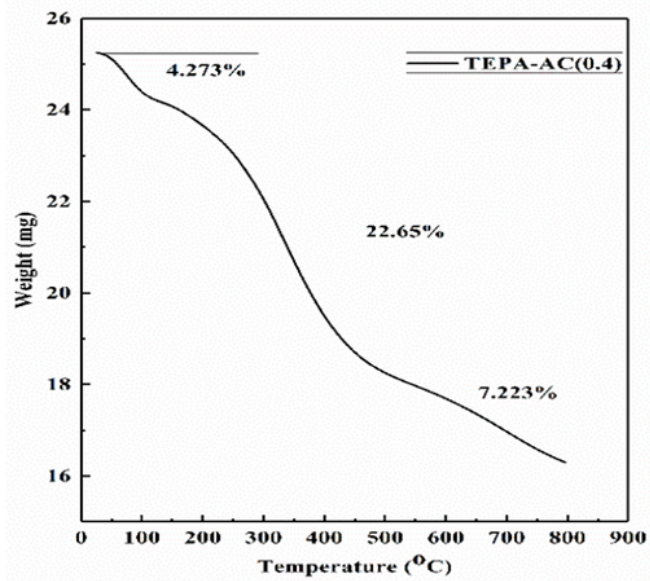


(b)

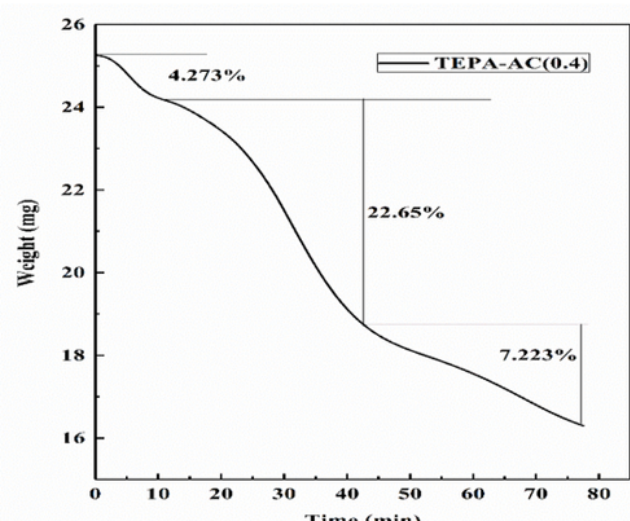
Figure 13

a) TGA for DEA-AC (0.4) (Weight Vs Temperature))

(b) TGA for TEPA-AC (0.4) (Weight Vs Time)



(a)



(b)

Figure 14

(a) TGA for TEPA-AC (0.4) (a) (Weight Vs Temperature)

(b) TGA for TEPA-AC (0.4) (b) (Weight Vs Time)

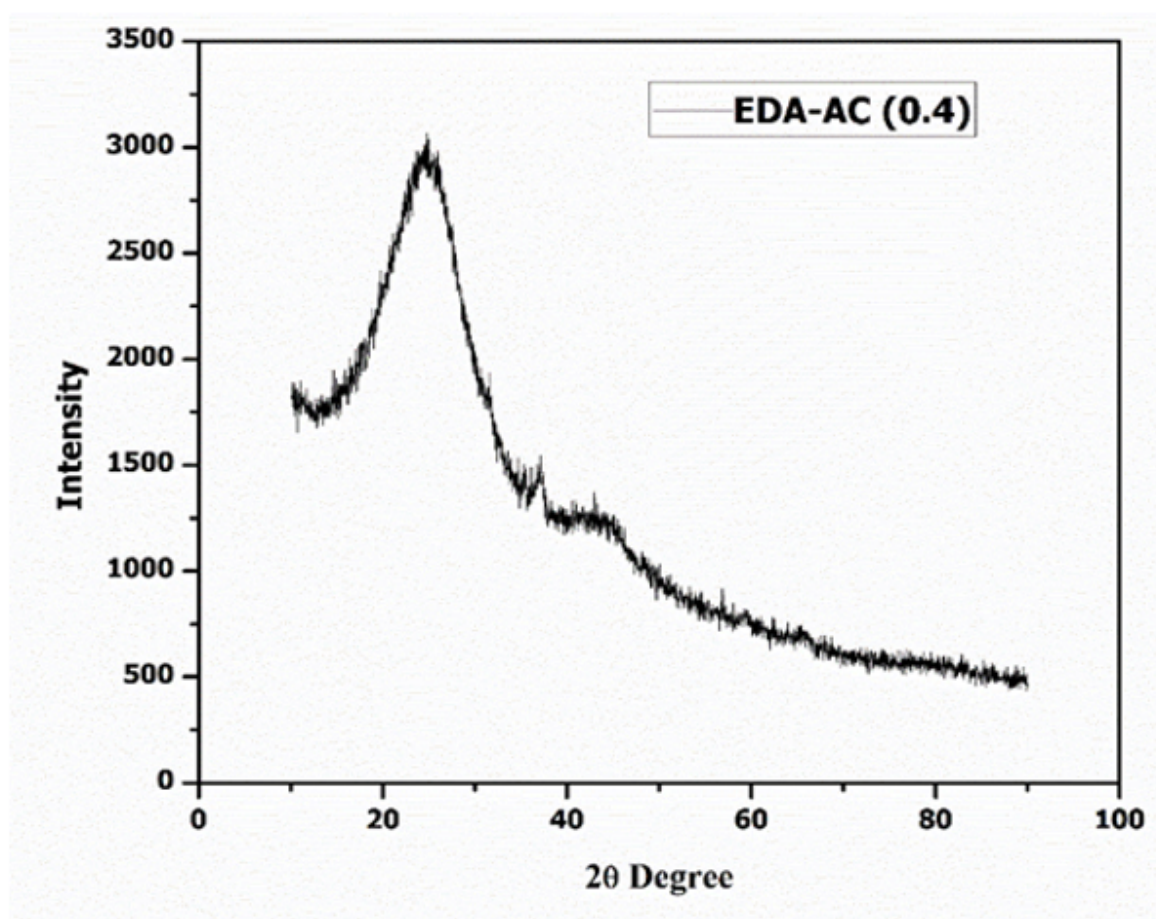


Figure 15

XRD Analysis of EDA-AC (0.4)

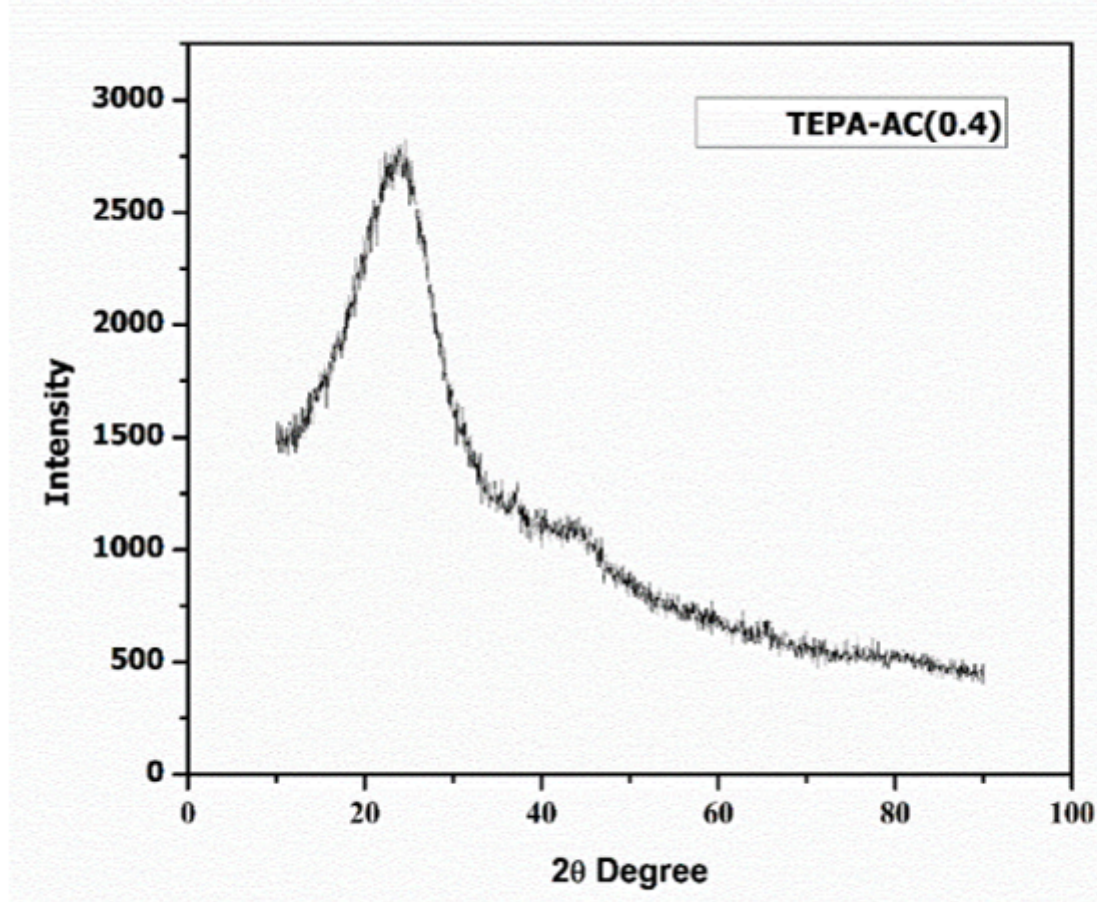


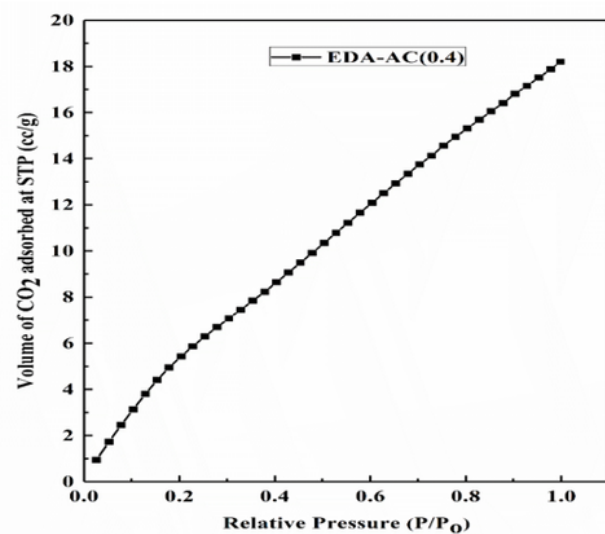
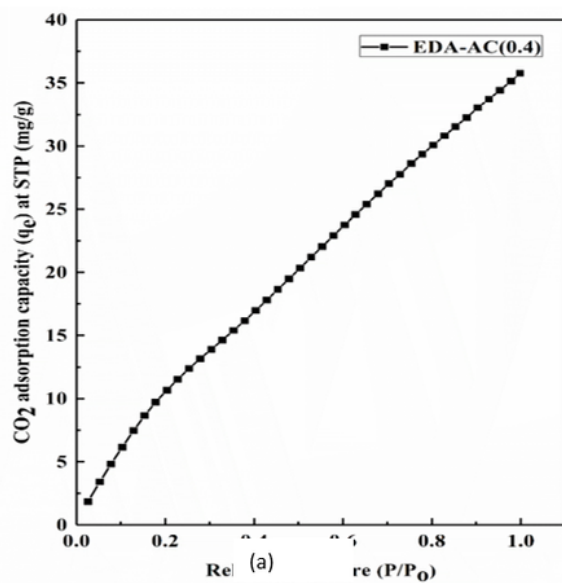
Figure 16

XRD Analysis of TEEA-AC (0.4)



Figure 17

Autosorb iQ Instrument for CO₂ Adsorption Analysis

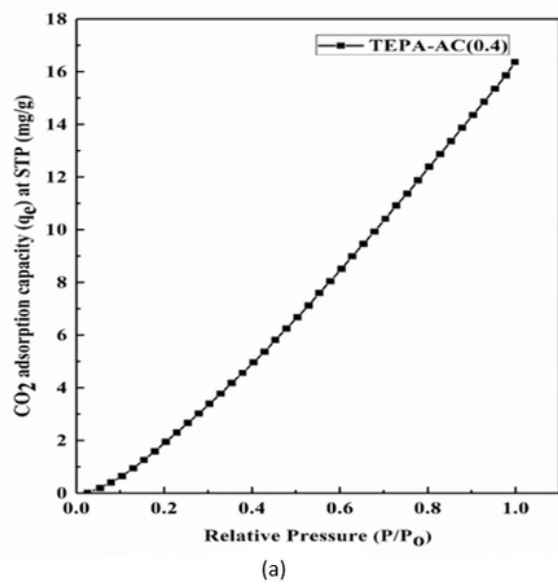


(b)

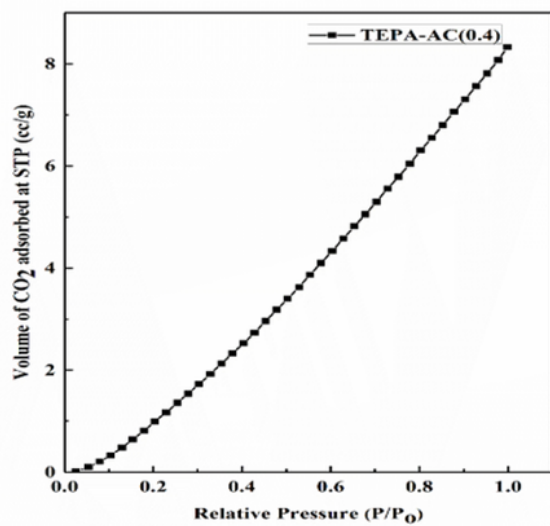
Figure 18

(a) CO_2 adsorption vs Relative pressure for EDA-AC (0.4)

(b) Volume of the CO_2 adsorbed vs Relative pressure for EDA-AC(0.4)



(a)



(b)

Figure 19

(a) CO₂ adsorption vs Relative pressure for TEPA-AC (0.4)

(b) Volume of the CO₂ adsorbed vs relative pressure for TEPA-AC (0.4)

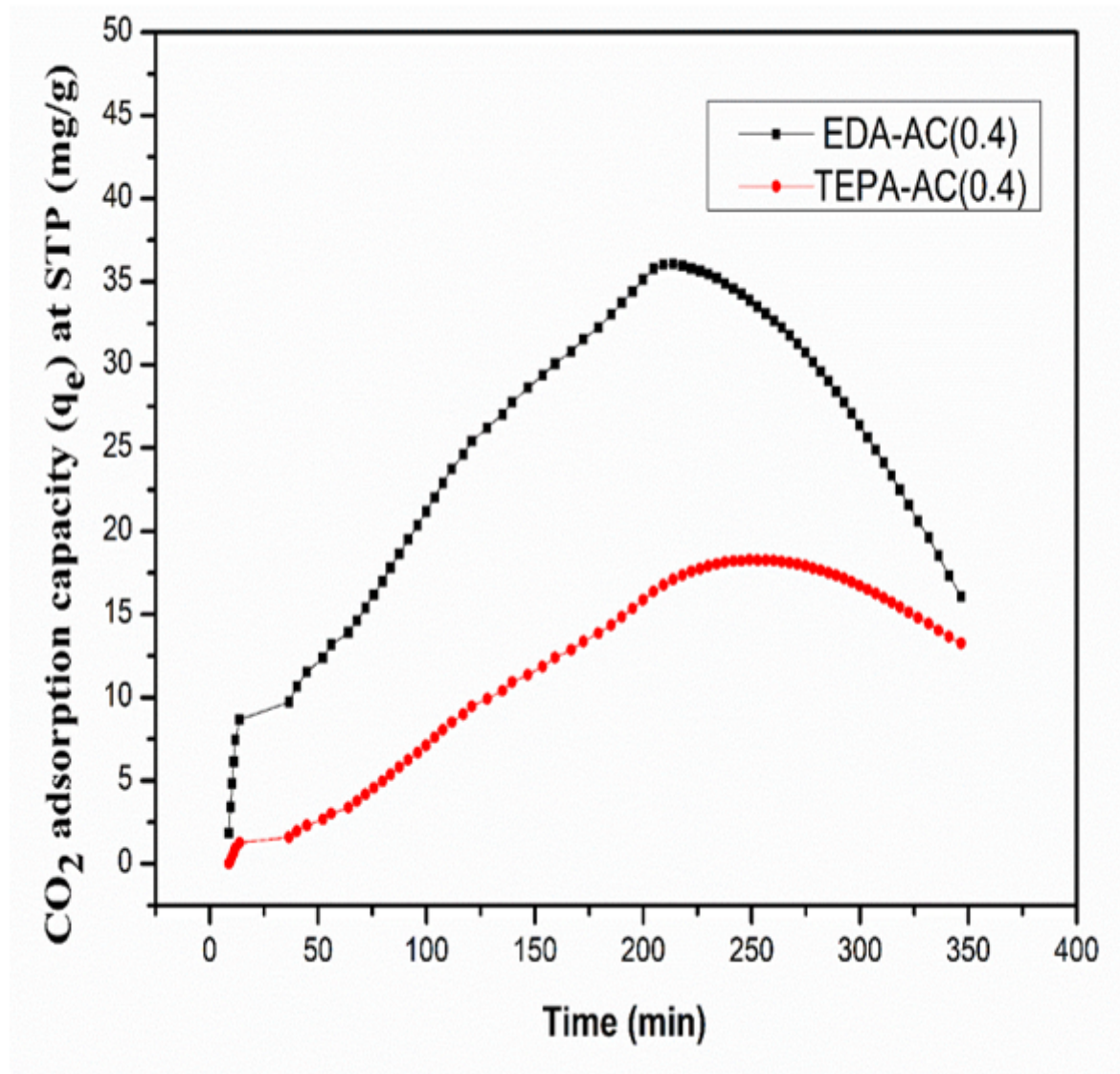


Figure 20

Breakthrough curve of CO_2 adsorption